

Decomposition of Sm α -SiAlON Phases during Post-Sintering Heat Treatment

Rupeng Zhao & Yi-Bing Cheng*

Department of Materials Engineering, Monash University, Melbourne 3168, Australia

(Received 1 November 1995; revised version received 13 December 1995; accepted 5 January 1996)

Abstract

The microstructural characteristics and the phase assembly of Sm ($\alpha+\beta$)-SiAlON ceramics before and after post-sintering heat treatment at 1450°C have been investigated by scanning electron microscopy (SEM), transmission electron microscopy (TEM) and X-ray diffraction (XRD). Grain boundary glass crystallization and the α -SiAlON to β -SiAlON (i.e. α' to β') phase transformation were observed as the major phase transformations occurring during the heat treatment. TEM studies indicated that the α' to β' transformation process itself could produce a nano-sized liquid phase inside the SiAlON grains, which could facilitate the transformation. Based on these observations, it is proposed that the α' to β' phase transformation in Sm SiAlONs is essentially a self-decomposition process of α' phases and may be described as:



Therefore, for an unstable α' phase, it would decompose, i.e. proceed $\alpha' \rightarrow \beta'$ transformation without having to involve large amounts of grain boundary liquid. However, the existence of the grain boundary liquid and β' grains as nuclei could reduce the activation energy barrier and accelerate the α' decomposition. © 1996 Elsevier Science Limited.

1 Introduction

Liquid phase sintering, using metal oxides and/or rare earth oxides as sintering additives, is commonly employed for densification of silicon nitride based ceramics. The oxides react with the silica on the surface of silicon nitride powder, resulting in the formation of an oxynitride liquid at sintering temperatures. This liquid phase assists densification but usually remains at grain boundaries as a

glassy phase upon cooling, which impairs the high-temperature mechanical properties of the material.^{1,2} Post-sintering heat treatment of SiAlON ceramics is used to crystallize the grain boundary glassy phase and subsequently improve the high-temperature properties of the materials.^{3,4} Recently, Mandal *et al.*⁵ revealed that some rare earth α -SiAlON (α') phases could undergo transformation to β -SiAlON (β') in the heat treatment temperature range between 1100 and 1550°C. α - and β -SiAlONs have different mechanical properties;⁶ therefore this discovery may open new routes for tailoring the microstructures and controlling the properties of ($\alpha+\beta$)-SiAlON ceramic composites.

The α' and β' phases have distinct compositions and possess different crystal structures.⁶ The transformation between α' and β' involves lattice reconstruction and requires a high degree of atomic diffusion. As a result of the strong covalent nature of the bonding associated with both the α' and β' structures, the atomic diffusivity of the species making up the lattices is inherently low. It is, therefore, generally assumed that the $\alpha' \rightarrow \beta'$ phase transformation requires a liquid phase to assist the necessary atomic diffusion, but the actual role of the liquid phase has not been fully understood. Recent experiments showed that the amount of grain boundary liquid phase in the sample had marked effects on the transformation, and the introduction of an additional amount of glass into a previously stable α' composition could significantly destabilize the α' phase and promote the $\alpha' \rightarrow \beta'$ transformation.⁷ Comparing the results in different rare earth SiAlON systems, Mandal and Thompson⁷ suggested that the residual grain boundary liquid phase was one of the most important factors influencing the transformation; the rate of the transformation depended mainly on the amount and viscosity of the intergranular liquid phase present during the heat treatment. Shen *et al.*,⁸ on the other hand, proposed two possible transformation

*To whom correspondence should be addressed.

routes, one involving a liquid phase, i.e. $\alpha' + \text{liquid} \rightarrow \beta' + \text{M}'$ and the other being a direct decomposition of the α' phase to form β' and the aluminium-containing melilite ($\text{Sm}_2\text{Si}_{3-x}\text{Al}_x\text{O}_3 + x\text{N}_{4-x}$, M')⁹ phases in the Sm ($\alpha+\beta$)-SiAlON system, without the involvement of a liquid phase.

In the present work, X-ray diffraction (XRD), scanning electron microscopy (SEM) and transmission electron microscopy (TEM) are used in the study of the $\alpha' \rightarrow \beta'$ transformation and the associated microstructural changes taking place in isothermal heat treatments at 1450°C. The involvement of liquid phase in the transformation at different stages of heat treatment is assessed through microstructural observations and analyses.

2 Experimental

Samples were pressureless sintered at 1820°C in a nitrogen atmosphere for 4 h, from Si_3N_4 , AlN, Al_2O_3 and Sm_2O_3 powders with a starting composition (in wt%) of 72.50 Si_3N_4 , 14.27AlN, 2.00 Al_2O_3 and 11.23 Sm_2O_3 . Full details of the sample preparation can be found in Ref. 9. XRD analyses revealed that the as-sintered materials contained mainly α' and β' phases and a trace of the 21R polytypoid phase. An amorphous grain boundary phase was also observed in the sample by electron microscope.

The sintered specimen was subsequently heat-treated at 1450°C for a total of 360 h in an alumina tube furnace in flowing high purity nitrogen, with both heating and cooling rates being 3°C min⁻¹. The heat treatment procedure was as follows: after the first 24 h of heat treatment at 1450°C, the sample was cooled down to room temperature and characterized using XRD, SEM and TEM; the same specimen was then reheated to 1450°C for another 36 h, making a total heat treatment time of 60 h. This procedure was repeated five times for the same sample with an interval of 60 h until the total heat treatment time reached 360 h. Three TEM specimens were prepared from the as-sintered sample, and from samples heat-treated for a total of 24 and 120 h. The purpose of this procedure was to ensure that all results were obtained from the same sample, so that any difference in crystalline phases observed can be mainly attributed to the heat treatment process. A thin oxidation layer appeared on the surface of the sample after each heat treatment, which was completely removed by grinding on SiC paper before XRD and SEM examinations.

Specimens for TEM study were carefully cut from the bulk of the sample and were mechanically ground, dimpled to a thickness of ~20 μm , and then

ion-milled to electron transparency. All specimens were carbon-coated before TEM and SEM studies to avoid surface charging. XRD was performed using a Rigaku X-ray diffractometer. The relative amount of α' and β' phases, i.e. the $\beta':(\alpha'+\beta')$ weight ratio, was measured using the calibration curves developed by Liddell¹⁰ with the intensities of both the α' and β' phases. Micro-structural observations were carried out on a Jeol 840A SEM and a Philips CM20 TEM equipped with an ultrathin-window EDS system.

3 Results

3.1 Rate of the α' to β' transformation

The α' phase was the predominant phase in the as-sintered sample with a $\beta':(\alpha' + \beta')$ weight ratio of 11%. Figure 1 shows the XRD patterns of the sample after the heat treatment at 1450°C for various durations. The intensities of the characteristic α' peaks decreased continuously with heat treatment time, whereas β' peak intensities increased. After 240 h, the proportion of the β' phase reached 85 wt% and α' eventually became a minor phase in the sample. This is clear evidence of $\alpha' \rightarrow \beta'$ transformation during the isothermal heat treatment. Accompanying this transformation was the formation of M' phase, which was a combined result of grain boundary glass devitrification⁹ and the $\alpha' \rightarrow \beta'$ transformation.^{8,11} Quantified $\beta':(\alpha'+\beta')$ ratios are presented in Fig. 2, in which the different rates of increase in $\beta':(\alpha'+\beta')$ have separated the heat treatment process into several stages. In the first 24 h, the amount of β' increased rapidly. Between 24 and 240 h, the rate of increase in β' was reduced but nearly maintained as a constant. After 240 h, the rate was further slowed down.

A total of 20 wt% increase in β' was found in the initial 24 h, giving an average rate of β' increase of around 0.8 wt% per hour. As pointed out in a previous paper,¹¹ the simultaneous grain boundary glass crystallization taking place at the same temperature in the initial few hours of the heat treatment could contribute to the increase in the $\beta':(\alpha'+\beta')$ ratio. About 7 vol% (i.e. ~11 wt%) of grain boundary glass was detected using an SEM image analyser in the as-sintered sample. Even if taking an overestimation that half of this glass (~5 wt%) crystallized to form β' , the average rate increase in the $\beta':(\alpha'+\beta')$ ratio resulting from the α' to β' transformation in the initial 24 h would still be greater than 0.6 wt% per hour. This figure is notably higher than that of the subsequent stages, indicating the significance of the grain boundary glass (liquid at 1450°C) in facilitating the $\alpha' \rightarrow \beta'$ transformation. Between 24 and

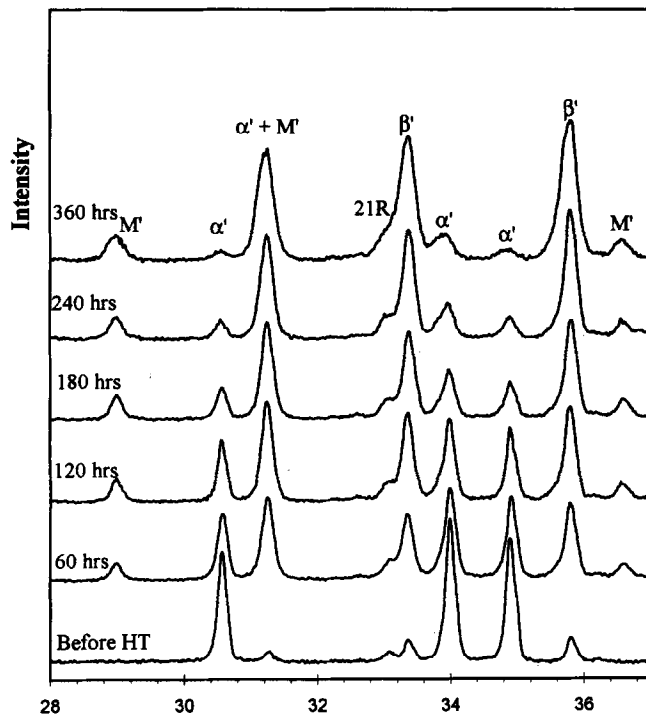


Fig. 1. XRD patterns for the Sm (α + β)-SiAlON specimen after heat treatment at 1450°C for a total of up to 360 h.

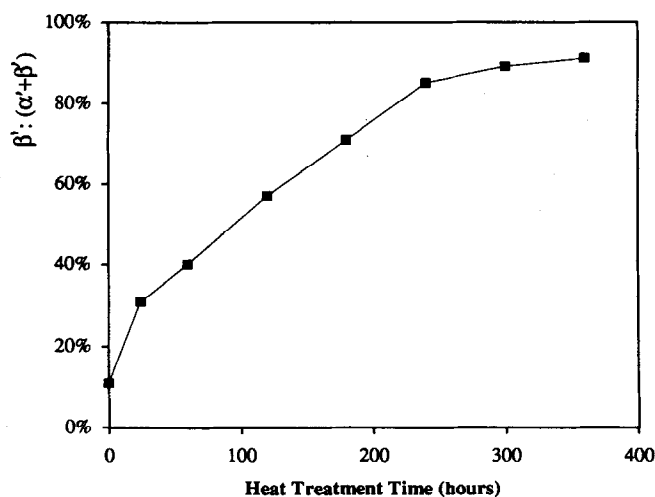


Fig. 2. The $\beta':(\alpha'+\beta')$ ratio of the samples heat-treated at 1450°C as a function of heat treatment time.

240 h, the $\beta':(\alpha'+\beta')$ ratio increased from 31 to 85 wt% with an almost constant rate of 0.2 wt% per hour. The marked reduction in the rate of β' increment at this stage corresponds to the fact that most of the glassy phase has crystallized after the early heat treatment. Further extension of the heat treatment time up to 360 h resulted in only a slight increase (~ 0.05 wt% per hour) in the $\beta':(\alpha'+\beta')$ ratio, indicating that the system was approaching an equilibrium state.

3.2 Devitrification of the grain boundary glass

The microstructure of the samples before and after the heat treatment was investigated by TEM. Figure 3 shows typical bright-field and dark-field

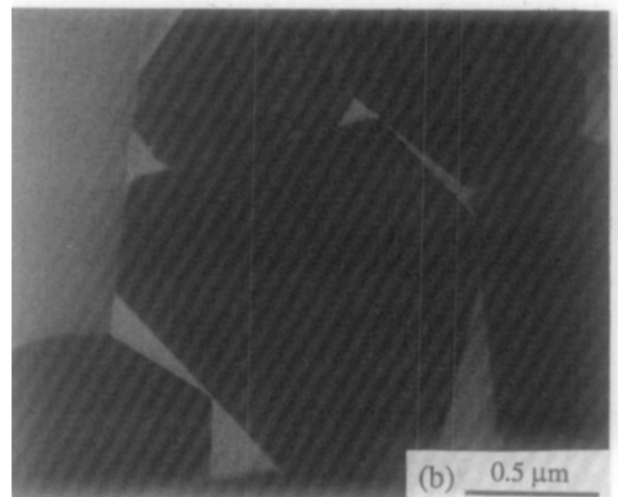
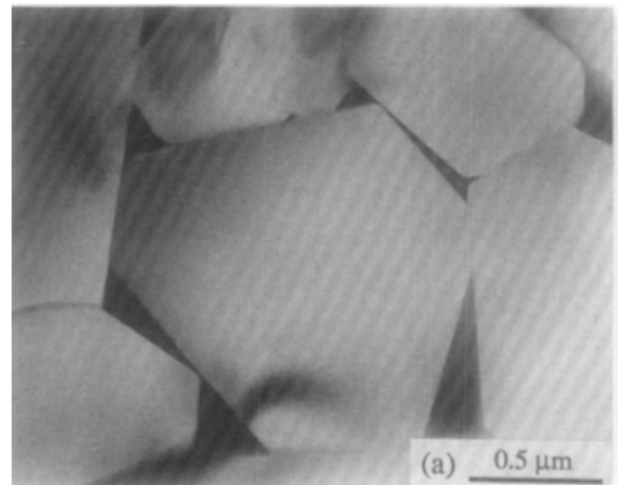


Fig. 3. TEM (a) bright-field and (b) diffused dark-field images from the as-sintered specimen.

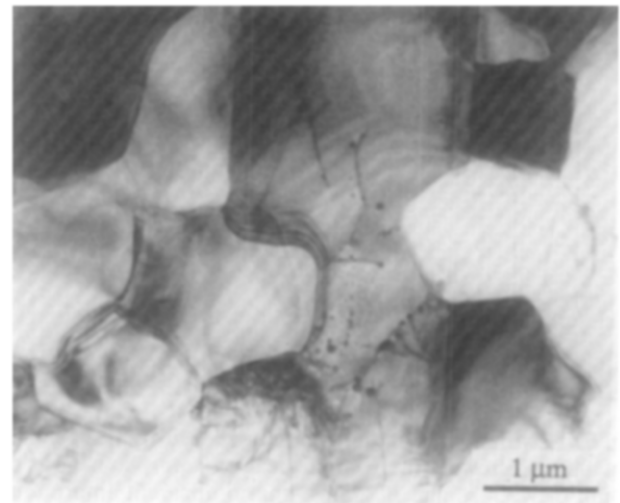


Fig. 4. Typical TEM bright-field image of the sample heat-treated at 1450°C for 24 h.

images of the as-sintered sample. In the bright-field image, the glassy phase appears darker because of its high Sm content, whereas in the diffused dark-field image, the glassy phase appears brighter.¹² It can be seen from Fig. 3 that in addition to the large glassy pockets at multiple grain junctions, every grain in the material is

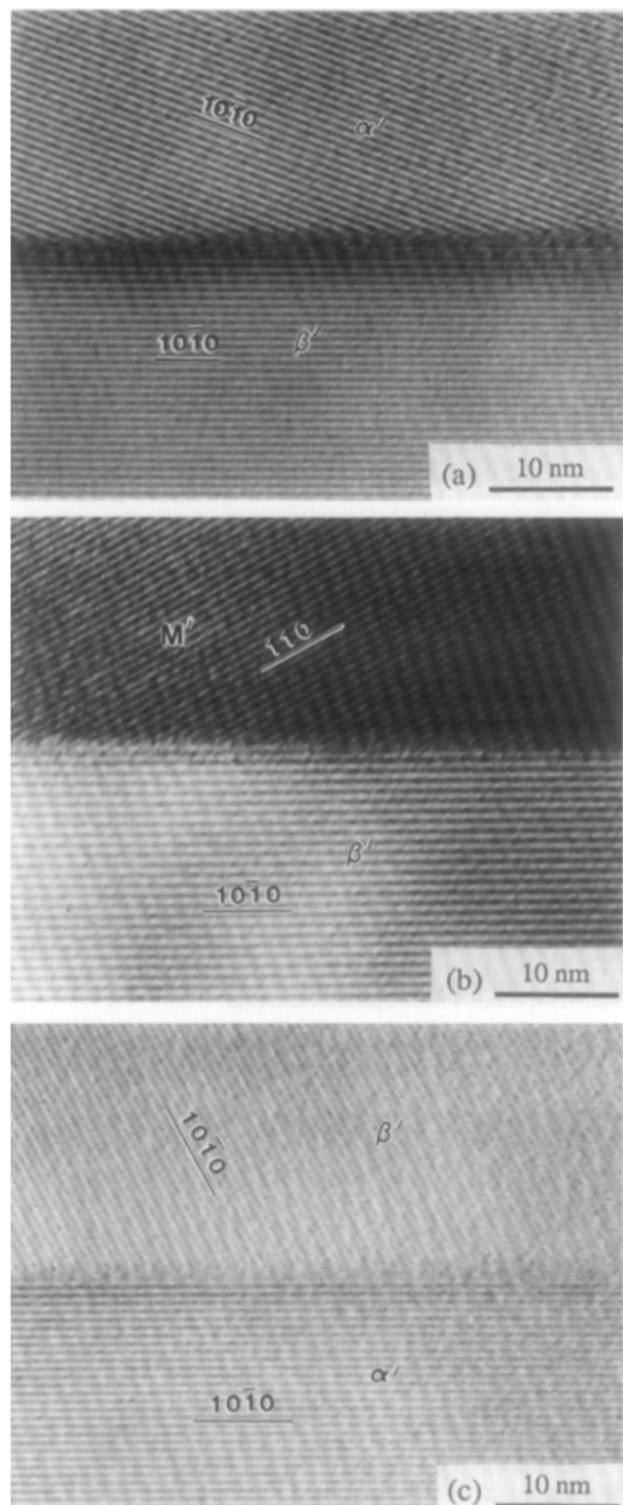


Fig. 5. TEM lattice images of the sample heat-treated for 120 h at 1450°C showing (a) in some areas an amorphous layer of ~ 1 nm between α' and β' grains; but no apparent amorphous layer is observed (b) between β' and M' grains, and (c) between α' and β' grains in other areas.

surrounded by an amorphous layer, suggesting that the liquid phase forms a three-dimensional interconnected network during sintering. Crystallization of the glassy phase was observed in the sample after heat treatment at 1450°C for 24 h. Extensive TEM observations indicated that all glassy multiple junctions in the samples were crystallized, giving M' as a stable grain boundary phase.¹¹ A

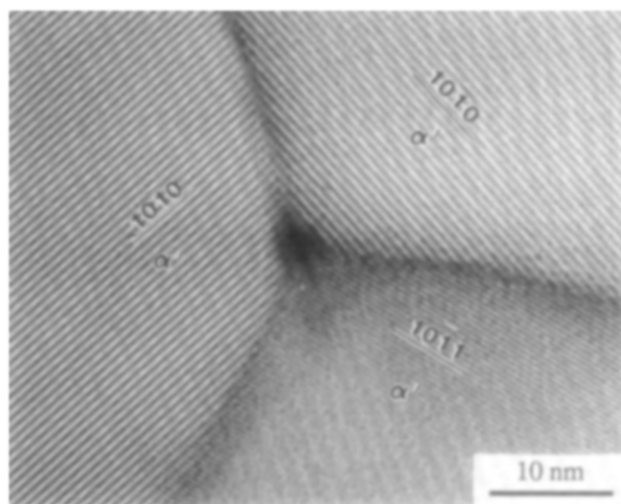


Fig. 6. TEM lattice image of a triple junction among three α' grains, showing a ~ 2 nm triple pocket in the sample heat-treated for 120 h at 1450°C.

typical bright-field image is shown in Fig. 4. Details of the grain boundaries were further studied by lattice imaging on the samples heat-treated for 24 and 120 h. The results from both samples revealed that, in some areas, an amorphous layer of ~ 10 Å was observed between SiAlON grains [as shown in Fig. 5(a)], consistent with other observations in silicon nitride ceramics.¹³ In other areas, however, no apparent amorphous layer was found [Figs 5(b) and (c)]. The size of the multi-grain pockets was reduced to around 20 Å after the heat treatment (Fig. 6). These observations suggest that post-sintering heat treatment above the eutectic temperature of the system has the potential to fully remove the glassy interface in SiAlON materials.⁹

From the TEM study, the amount of remaining grain boundary glass is very limited after the heat treatment at 1450°C for 24 h. Even assuming that all grains in the heat-treated material are still surrounded by a residual amorphous film 10 Å thick, for a sample with an average grain size of ~ 1.5 μm it is estimated that the actual volume percentage of this residual glassy phase should not be greater than 0.3%. It is thought that such a small amount of grain boundary glass may only have a very limited role to play in the subsequent α' to β' transformation process.

3.3 Evidence of self-generated liquid in the transforming α' phase

Because of the strong covalent bonding in both α' and β' phases, the atomic diffusivity of the species in SiAlON structures would be extremely low without the assistance of a liquid phase. TEM microstructural study¹⁴ revealed that the transformed β' grains in a sample heat-treated for 120 h have unique microstructural features consisting of a high density of dislocations and nano-sized spherical inclusions (Fig. 7). The inclusions are

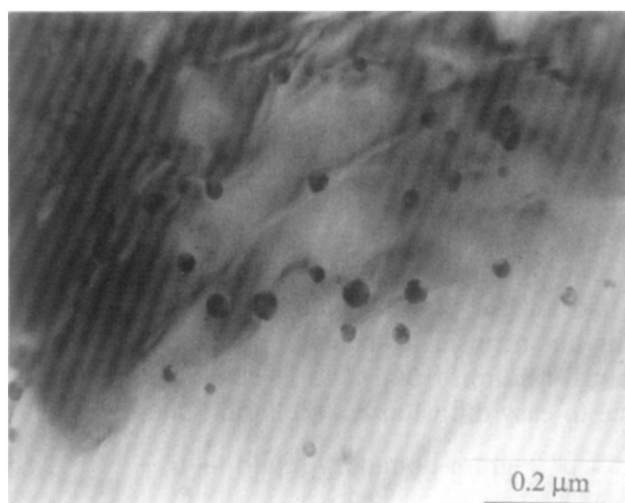


Fig. 7. TEM image of nano-sized spherical inclusions within a transformed β' grain. The area fraction of the inclusions in this area was 6%, corresponding to a volume fraction of 2.5%. The sample was heat-treated at 1450°C for 120 h.

often closely associated with dislocations and rich in Sm, coinciding with the expectation that the $\alpha' \rightarrow \beta'$ transformation requires the rejection of the stabilizing cation (Sm^{3+} in the present case) from the α' lattice. The perfect spherical shape of these inclusions implied that they were of a liquid nature at the heat treatment temperature. Similar microstructural features have also been observed in the sample heat-treated for 24 h. Figure 8 is an enlargement of a grain in Fig. 4 and shows bright-field and diffused dark-field images of a β' grain containing many spherical inclusions. It can be seen that most inclusions in a widely dispersed area appeared brighter in the diffused dark-field image [Fig. 8(b)], indicating the possible amorphous status of these inclusions. Because there is no mechanism for the β' phase to accommodate the Sm-rich inclusions inside its structure, it is postulated that the spheroid-containing β' grain is virtually the one that has transformed from an α' structure, and the nano-sized inclusions are liquid regions produced as a result of the rejection of Sm species from the original α' grain. The exact mechanism of this local liquid phase formation is unclear at this stage and deserves further investigation. In this paper, the dispersed liquid phase found inside the SiAlON grains is referred to as the *self-generated liquid* to distinguish it from the grain boundary liquid formed during sintering.

The volume percentage of these inclusions in the area shown in Fig. 7 is around 2.5%, estimated on the basis of the measured thickness of the specimen and the area fraction of the inclusions in the image. The quantity of this internal self-generated liquid in local areas is significantly higher than that of the residual glass at grain boundaries. Therefore it is expected that the self-generated liquid phase would play a more active role in

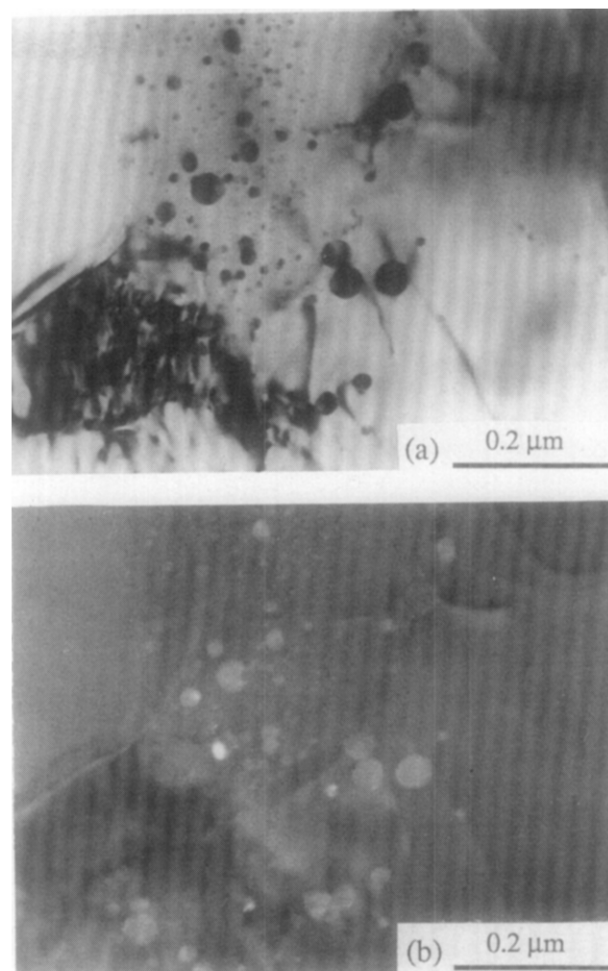


Fig. 8. TEM (a) bright-field and (b) diffused dark-field images of inclusions in the sample heat-treated for 24 h at 1450°C. The brighter contrast of the inclusions in the diffused dark-field image suggests that they are of an amorphous nature.

facilitating the $\alpha' \rightarrow \beta'$ transformation after the grain boundary crystallization. Although the inclusion-containing β' grains are commonly observable in these samples, it is generally true that they do not appear in a great quantity and tend to be isolated by less characteristic SiAlON grains of both α' and β' forms (Fig. 4), which corresponds to a very sluggish transformation process (<1 wt% per hour). It is not exactly clear how this type of microstructure has developed at the moment, but it may denote the importance of suitable nucleating sites to the transformation.

4 Discussion

4.1 Involvement of the grain boundary liquid in the transformation

The observation of $\alpha' \rightarrow \beta'$ transformations in rare earth SiAlON systems has indicated the unstable characteristic of some α' compositions in a certain temperature range. However, the strong covalent bonding in both the α' and β' lattices and the reconstructive nature of this phase transformation may prevent the process from occurring

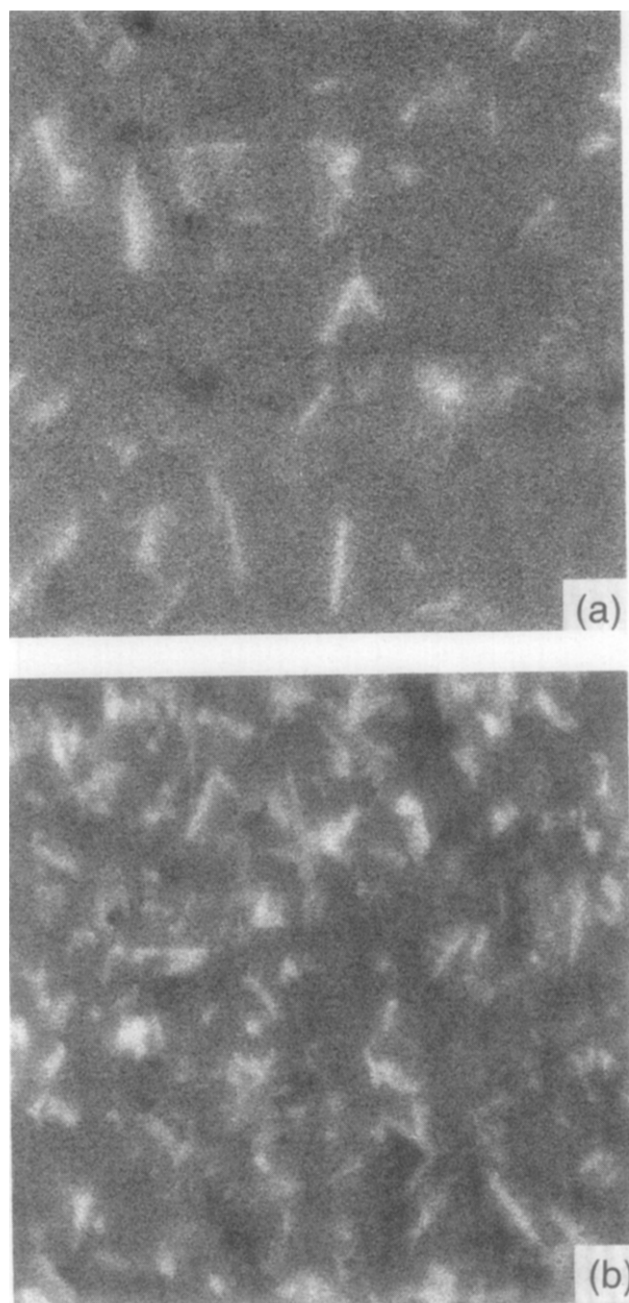


Fig. 9. EDS Al X-ray maps of (a) the as-sintered sample and (b) the sample heat-treated for a total of 360 h at 1450°C. The bright regions in the Al X-ray maps correspond to the 21R phase ($\text{SiAl}_6\text{O}_2\text{N}_6$), which has the highest Al concentration in the material.

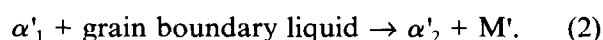
if the material was fast cooled or if no liquid phase existed to assist the necessary atom diffusion. On the other hand, there is always a glassy phase remaining at SiAlON grain boundaries after liquid phase sintering. This glass is a supercooled oxynitride liquid and softens above the glass transition temperature (T_g), ranging between 900 and 1000°C.⁵ The viscosity of a liquid phase drops exponentially with increasing temperature above the T_g ,¹⁵ and it is thought that the grain boundary liquid would become very reactive at 1450°C. Although melting of the grain boundary glass may not ensure an $\alpha' \rightarrow \beta'$ phase transformation, it

would promote chemical reactions between molten glass and α' phases, modifying the α' compositions, and foster lattice diffusion.

The active involvement of the grain boundary liquid in the transformation process is marked by the highest $\alpha' \rightarrow \beta'$ transformation rate achieved in the initial 24 h of heat treatment (Fig. 2). Two types of reactions involving both the grain boundary liquid and α' phases could take place at 1450°C. For an intrinsically unstable α' composition, the transformation from α' to β' could be accelerated due to easy diffusion via the liquid phase.^{8,16,17}



whereas for a stable α' phase, its composition may be altered through a chemical reaction:⁸



The stability of the α'_2 phase is dictated by the new composition as well as the continuing reaction with the liquid. Obviously, a larger volume of the grain boundary liquid phase in the materials would greatly extend change the α' composition and even destabilize α' structures. This is in agreement with the reported experimental results.⁷

The interaction between the grain boundary liquid and SiAlON phases at 1450°C is also imperative for M' to form as a grain boundary crystalline phase. The maximum nitrogen concentration in an Sm oxynitride glass is about 40 eq%.¹⁸ Both reactions (1) and (2) could lead to an increase in the N content of the liquid from which the M' phase, containing 53 eq% nitrogen, could precipitate.⁹ The M' phase has a high Sm content and it is more stable than some of the α' compositions at the heat treatment temperature. As a result, the formation of M' provides an additional driving force for the $\alpha' \rightarrow \beta'$ transformation. It becomes clear from the above discussion that the volume and the viscosity of the grain boundary liquid phase can markedly affect the $\alpha' \rightarrow \beta'$ transformation process at the initial stage of heat treatment when the grain boundary crystallization is not yet complete.

4.2 Role of the self-generated liquid in the transformation

After the initial period of heat treatment (e.g. $t > 24$ h), the volume percentage of the residual grain boundary glass is reduced from ~7 vol% to <0.3 vol%, hence its role in the transformation would be severely restricted. Moreover, the M' phase is very stable at 1450°C; once it has formed, it would not remelt to become a grain boundary liquid phase and to be involved in the $\alpha' \rightarrow \beta'$ transformation at this temperature.^{8,9} The rate of the $\alpha' \rightarrow \beta'$ transformation at the second stage ($24 < t$

< 240 h) is lower than that at the first stage ($t < 24$ h) but the process continues at a nearly constant rate, suggesting an additional mechanism(s) to be operative. The activation energy of a reconstructive phase transformation will be significantly reduced if the atomic diffusion is assisted by a liquid phase and/or if there exist nuclei to reduce the interfacial energy. The occurrence of the self-generated liquid in transformed β' grains leads to a logical assumption that this liquid phase may have played a major role in promoting atomic diffusion and facilitating $\alpha' \rightarrow \beta'$ transformation after crystallization of the grain boundary liquid. Because it involves a liquid phase emerging from the transforming α' phase itself, the transformation from α' to β' can proceed without involving much grain boundary liquid and a steady rate of the transformation is expected. This is in agreement with the experimental observation. The appearance of the Sm-rich spheroids in the β' phase results in thermodynamic instability, hence these nano-sized inclusions would eventually diffuse out of the transformed β' grains through the easy path of dislocations. It is, therefore, suggested that the amount and viscosity of the self-generated liquid within the transforming α' grains is a determining factor in controlling the rate of the $\alpha' \rightarrow \beta'$ transformation when most of the grain boundary glass has been crystallized.

4.3 Decomposition of α -SiAlON phases

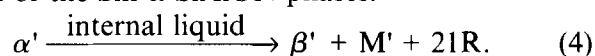
Without much involvement of grain boundary glass, the $\alpha' \rightarrow \beta'$ transformation at the second stage may be regarded as a decomposition process of α -SiAlON phases. This suggests that, below a certain temperature, some of the α' compositions have a higher free energy than β' phases, and the transformation from α' to β' would occur if it could be thermally activated. Because of the compositional difference between α' and β' phases, the decomposition of an α' phase must produce other phase(s) in addition to a β' composition. Shen *et al.*⁸ suggested a possible route for this reaction:



which seemed reasonable according to the XRD observations (Fig. 1). If the actual compositions of all the phases involved are considered, however, the proposed reaction (3) would yield excessive amounts of Al and N. To balance the compositions, therefore, one has to assume the formation of AlN polytypoid in addition to the β' and M' phases. AlN polytypoids are compatible with α' , β' and M' phases in the Sm and Nd SiAlON systems,¹⁹ and the 21R polytypoid phase was

commonly observed in the present samples before and after heat treatments.

There are some experimental difficulties in quantifying the AlN polytypoid phase by using the XRD and SEM backscattered imaging techniques. Almost all the XRD peaks of the 21R polytypoid strongly overlap with those of α' , β' or M' phases, and there are no detectable differences between the polytypoid and β' phases in SEM backscattered images because of the similar atomic weights of Si and Al elements. For these reasons, there have been few reports on the quantification of AlN polytypoid phases in the literature. Nevertheless, our recent study has showed that it is possible to analyse the amount of the 21R polytypoid phase by using the EDS X-ray mapping technique. Details of this work will be reported elsewhere.²⁰ Figure 9 shows the Al X-ray maps from the (a) as-sintered and (b) 360 h heat-treated samples. The bright regions in the Al maps correspond to the 21R phase ($\text{SiAl}_6\text{O}_2\text{N}_6$), which has the highest Al concentration among all phases in the samples. It can be seen that the amount of the 21R phase increases considerably after the heat treatment, which cannot be simply accounted for the grain boundary glass devitrification. The increase in the 21R phase appearing in the XRD profiles (Fig. 1) is not as clear as that showed in the X-ray maps and the difference is not fully understood at the present time. Considering the strong overlap in the XRD peaks and the excellent resolution of the characteristic X-ray maps, however, it is plausible to conclude that the AlN polytypoid phase is also a product of the $\alpha' \rightarrow \beta'$ phase transformation. With this result and the observed self-generated liquid phase, a new reaction path is proposed for the decomposition of the Sm α -SiAlON phases:



It is suggested that an unstable α' phase could decompose into a β' phase plus M' and 21R polytypoid, and the process is assisted by the self-generated liquid phase formed during the decomposition. It is thought that the α' decomposition is a dominant phenomenon proceeding during this phase transformation and the grain boundary glass is mainly involved in the initial stage of the process. From this point of view, the $\alpha' \rightarrow \beta'$ transformation may be considered as a part of the story of the α' phase decomposition.

5 Conclusions

Some of the Sm α -SiAlON compositions are thermodynamically unstable and may decompose at

elevated temperatures (e.g. 1450°C). The result of this decomposition appears most prominently in the form of the $\alpha' \rightarrow \beta'$ transformation, although other phases have also been produced. At the initial stage, the decomposition process is assisted by the grain boundary liquid phase and progresses readily. When most of the grain boundary glass is crystallized, the rate of this decomposition becomes much slower but is maintained roughly constant until the system is close to equilibrium. The α' decomposition produces a self-generated liquid phase inside the SiAlON grains, which could in turn facilitate atom diffusion. The final products of the α' decomposition include β' , M' and 21R polytypoid phases.

Acknowledgement

This work was supported by the Australian Research Council.

References

1. Jack, K. H., Review: SiAlONs and related nitrogen ceramics. *J. Mater. Sci.*, **11** (1976) 1135–58.
2. Ekström, T. & Nygren, M., SiAlON ceramics. *J. Am. Ceram. Soc.*, **75** (1992) 259–76.
3. Lewis, M. H., Crystallisation of grain boundary phases in silicon nitride and SiAlON ceramics. In *Silicon Nitride 93, Key Engineering Materials Vol. 89–91*, eds M. J. Hoffmann, P. F. Becher & G. Petzow. Trans Tech Publ. Switzerland, 1993, pp. 333–8.
4. Thompson, D. P., New grain boundary phases for nitrogen ceramics. In *MRS Symposium Proceedings Vol. 287, Silicon Nitride Ceramics — Science and Technological Advances*, eds I-Wei Chen et al. MRS, Pittsburgh, PA, 1993, pp. 79–92.
5. Mandal, H., Thompson, D. P. & Ekström, T., Reversible $\alpha \leftrightarrow \beta$ SiAlON transformation in heat-treated SiAlON ceramics. *J. Eur. Ceram. Soc.*, **12** (1993) 421–9.
6. Hampshire, S., Nitride Ceramics, In *Materials Science and Technology, Vol. 11 Structure and Properties of Ceramics*, ed. M. Swain. VCH, Weinheim, 1994, pp. 121–71.
7. Mandal, H. & Thompson, D. P., Mechanisms for α to β -SiAlON transformation. *Proc. 4th Conf. Eur. Ceram. Soc. Conf.*, Italy, 1995, pp. 327–34.
8. Shen, Z. J., Ekström, T. & Nygren, M., Temperature stability of samarium doped α -SiAlON ceramics. *J. Eur. Ceram. Soc.*, **16** (1996) 43–54.
9. Cheng, Y.-B. & Thompson, D. P., Preparation and grain boundary heat-treatment of samarium α -SiAlON ceramics. *J. Eur. Ceram. Soc.*, **14** (1994) 13–21.
10. Liddell, K., "X-ray analysis of nitrogen ceramic phases." M.Sc. Thesis, University of Newcastle upon Tyne, 1979.
11. Zhao, R. & Cheng, Y.-B., Phase transformation in Sm ($\alpha + \beta$)-SiAlON ceramics during post-sintering heat treatments. *J. Eur. Ceram. Soc.*, **15** (1995) 1221–8.
12. Clark, D. R., On the detection of thin intergranular films by electron microscopy. *Ultramicroscopy*, **4** (1979) 33–44.
13. Kleebe, H. J., Cinibulk, M. K., Cannon, R. M. & Ruhle, M., Statistical analysis of intergranular film thickness in silicon nitride ceramics. *J. Am. Ceram. Soc.*, **76** (1993) 1969–77.
14. Zhao, R., Cheng, Y.-B. & Drennan, J., Microstructure features of the α to β -SiAlON phase transformation. *J. Eur. Ceram. Soc.*, **16** (1996) 529–34.
15. Paul, A., *Chemistry of Glasses*, Chapman and Hall, London, 1990.
16. Cheng, Y.-B., & Thompson, D. P., Aluminium-containing nitrogen melilite phases. *J. Am. Ceram. Soc.*, **77** (1994) 143–8.
17. Shen, Z. J., Ekström, T. & Nygren, M., Homogeneity region and thermal stability of neodymium doped α -SiAlON ceramics. *J. Eur. Ceram. Soc.*, in press.
18. Tu, H. Y., Sun, W. Y., Wang, P. L. & Yan, D. S., Glass-forming region in the Sm–Si–Al–O–N system. *J. Mater. Sci. Lett.*, **14** (1995) 1118–22.
19. Sun, W. Y., Yan, D. S., Gao, L., Mandal, H., Liddell, K. & Thompson, D. P., Subsolvus phase relationships in the systems Ln_2O_3 – Si_3N_4 – AlN – Al_2O_3 (Ln = Nd, Sm). *J. Eur. Ceram. Soc.*, **15** (1994) 349–55.
20. Zhao, R. & Cheng, Y.-B., The formation of AlN polytypoid phases during α -SiAlON decomposition. *J. Am. Ceram. Soc.*, submitted.